

Study of β^+ /EC-decay properties of sd shell nuclei using nuclear shell model

Surender¹, Vikas Kumar^{1a}, Praveen C. Srivastava^{2b}

¹Department of Physics, Institute of Science, Banaras Hindu University Varanasi, Varanasi - 221 005, INDIA

²Department of Physics, Indian Institute of Technology Roorkee, Roorkee 247 667, INDIA

October 10, 2024

Abstract. Our study employs the nuclear shell model to systematically compute the half-lives of β -decay for nuclei in the mass range of $A = 18 - 39$, encompassing the majority of sd shell nuclei. This analysis utilizes the USDB and SDNN Hamiltonians. The theoretical outcomes contain calculations of various parameters such as Q -values, half-lives, excitation energy, $\log ft$ values, and branching ratios. We explore these results with axial-vector coupling constant for weak interactions, denoted as $g_A (= 1.27)$, and κ value ($= 6289$). We perform calculations of Gamow Teller matrix elements for 116 decay processes to calculate the quenching factor; we found a quenching factor of $q = 0.794 \pm 0.05$ for the USDB interaction and $q = 0.815 \pm 0.04$ for the SDNN interaction. We have also calculated superallowed transitions $0^+ \rightarrow 0^+$ for seven nuclei. Further, we have also included the electron capture phase space factor for the required nuclei to calculate the half-lives. This inclusion leads to small contribution in results, particularly for nuclei where electron capture (EC) plays a significant role. The overall results are in agreement with the experimental data.

PACS. 21.60.Cs Shell model, 23.40.-s β -decay

1 Introduction

The β^+ and EC -decay is the dominant mode of radioactive decay for unstable proton-rich nuclei; in β^+ -decay process a proton changes into a neutron and in EC -decay process inner orbital electron of atom is absorbed within the nucleus where it combines with a proton and forming a neutron and a neutrino [1]. The β -decay studies are important because we can get information on both nuclear structure and nuclear astrophysics [2, 3]. The nuclear shell model has successfully described various aspects of nuclear structure and beta decay properties of exotic nuclei [4]. The nuclear structure study of $N = Z$ nuclei in the nuclear chart is fascinating because these nuclei show several phenomena, such as shape coexistence along the $N = Z$ line and the role of pairing correlation of neutron and proton [5]. From the rp -process point of view, $N = Z$ nuclei are also important. In this work, we have used the nuclear shell model approach to study a theoretical understanding of observed β^+ -decay properties of 37 proton-rich and $N = Z$ nuclei of sd space. The present study is motivated with the availability of recent experimental data for β^+ -decay.

In Wilson *et al.* [6], the experimental Gamow-Teller β^+ and electron-capture decays of ^{14}O , ^{21}Na , ^{25}Al , ^{26}Si ,

^{29}P , ^{30}P , ^{30}S , ^{31}S , ^{33}Cl , ^{34}Cl , ^{35}Ar , ^{38}Ca , and ^{41}Sc nuclei have reported and compared with previous works. They also reported thirteen new observed branching ratios for these nuclei. The β^+ -decays of ^{18}Ne and ^{19}Ne and their relation to parity mixing in ^{18}F and ^{19}F is reported in [7]. The Gamow-Teller branching ratio and half-life in the β decay of ^{21}Na are outlined in [8]. The observed half-life and branching ratio of ^{21}Mg are reported in [9]. Experimental investigations on the half-lives and superallowed β decay of three nuclei, namely ^{18}Ne , ^{22}Mg , and ^{26}Si , were studied in [10]. Using the IGISOL facility at the University of Jyväskylä, half-lives and branching ratios of ^{23}Mg and ^{27}Si have been measured and reported in [11].

In Achouri *et al.* [12], the half-life of ^{22}Al was observed through β^+ decay process $^{22}\text{Al} \rightarrow ^{22}\text{Mg}$ at GANIL using LISE3 facility. In Warburton *et al.* [13] β^+ -decay of ^{24}Al has been studied, and a few new branches are also reported. The β decay properties of the neutron-deficient nuclei ^{25}Si and ^{26}P were explored at GANIL using the LISE3 facility [14]. Several weak branches are observed for ^{27}Si and ^{35}Ar β^+ -decay in Daehnick *et al.* [15]. The ft value of the superallowed $0^+ \rightarrow 0^+$ transition in β^+ -decay of ^{32}Ar has been discussed in [16]. The proton-rich nucleus ^{33}Ar has been studied through β^+ -decay using the SPIRAL facility at GANIL. In Iacob *et al.* [17], the β^+ -decay half-lives of ^{34}Ar and ^{34}Cl are measured and discussed in details. The β^+ decay half-life of neutron-deficient isotope ^{31}Cl was reported in [18]. First time the ^{35}K nucleus has

^a vikasphysics@bhu.ac.in

^b praveen.srivastava@ph.iitr.ac.in

been populated and its decay properties have been studied in [19]. The β decay of ^{37}K is studied in [20], and several new β decay branches are assigned to this nucleus. In Kaloskamis et. al. [21], the β^+ -decay properties of ^{37}Ca are reported. The β^+ -decay of ^{38}Ca and its branching ratios are observed using the LISE3 facility of GANIL in [22]. The β^+ decays of ^{39}Ca and ^{35}Ar were measured by using a Ge(Li) detector in [23].

In the present work first we have calculated the quenching factor for sd space using Gamow-Teller transition strength of β^+ -decay and then we did a comprehensive β^+ /EC -decay shell model study of 37 sd shell nuclei. Further, the calculated excitation energies, $\log ft$ -values, quenched half-lives, Q -values and branching ratios are compared with the available experimental data. In our previous work we have reported the shell model study of β -decay for fp and fp_g shell nuclei in [24, 25, 26], and β^+ /EC-decay study for $Z = 21 - 30$ shell nuclei in [27].

The section 2 consists of β^+ /EC-decay formalism, Q -value formalism, shell model Hamiltonian, model space, and quenching factor. The results and discussions are given in section 3. Finally, the summary and conclusions are drawn in section 4.

2 Details of the Shell Model Calculations

2.1 β -decay formalism

The observed Gamow Teller strength appears to be systematically smaller than what is theoretically expected on the basis of the model-independent Ikeda sum rule ‘ $3(N - Z)$ ’. The quench factor q in a given model space is calculated by averaging all ratios between the experimental and theoretical matrix elements $R(GT)$ values. The $R(GT)$ values are calculated using Gamow-Teller reduced transition probabilities $B(GT)$. Following Ref. [28], the Gamow-Teller reduced transition probabilities is given by

$$B(GT) = \left(\frac{g_A}{g_V}\right)^2 \langle \sigma\tau \rangle^2, \quad (1)$$

where the axial-vector coupling constant of the weak interactions is represented by g_A ($= 1.270$) and g_V ($= 1.0$) represents the vector coupling constant of the weak interaction. The Gamow-Teller operator $\langle \sigma\tau \rangle$ is given by

$$\langle \sigma\tau \rangle = \frac{\langle f || \sum_k \sigma^k \tau_{\pm}^k || i \rangle}{\sqrt{2J_i + 1}}, \quad (2)$$

where i and f represent the required quantum numbers to specify the initial and final states, respectively. The \pm refers to β^{\pm} decay, $\tau_{\pm} = \frac{1}{2}(\tau_x + i\tau_y)$ with $\tau_+ p = n$, $\tau_- n = p$. The total angular momentum of the initial state is represented by J_i .

The matrix elements $M(GT)$ are related to reduced transition probability $B(GT)$ as [29],

$$M(GT) = [(2J_i + 1)B(GT)]^{1/2}. \quad (3)$$

The ‘‘expected’’ total strength W can be used to normalize the matrix elements $M(GT)$ to get effective g_A . The total strength W is defined as

$$W = \begin{cases} |g_A/g_V| [(2J_i + 1)3|N_i - Z_i|]^{1/2}, & \text{for } N_i \neq Z_i, \\ |g_A/g_V| [(2J_f + 1)3|N_f - Z_f|]^{1/2}, & \text{for } N_i = Z_i, \end{cases} \quad (4)$$

The matrix elements $R(GT)$ are defined as

$$R(GT) = \frac{M(GT)}{W}. \quad (5)$$

The experimental $B(GT)$ values are calculated using experimental $\log ft$ values (listed in Table 1), the experimental $M(GT)$ values are obtained using Eq. 3.

In β^+ /EC-decay process, the mass number A remains unchanged, whereas the atomic number Z changes by one unit. The half-life ($t_{1/2}$) of β -decay is related to transition probability (T_{fi}) as

$$t_{1/2} = \frac{\ln 2}{T_{fi}}. \quad (6)$$

The consequential expression for total decay half-life of a combined β^+ and EC transition (represented by β^+ /EC) is given by

$$f_0 t_{1/2} = \left[f_0^{(+)} + f_0^{(EC)} \right] t_{1/2} = \frac{\kappa}{[g_A^2 * B(GT) + B(F)]}, \quad (7)$$

where f_0 is the phase-space factor (Fermi integral). The $B(F)$ is the Fermi reduced transition probabilities. The updated value of κ from literature [30] is given by

$$\kappa \equiv \frac{2\pi^3 \hbar^7 \ln 2}{m_e^5 c^4 (G_F \cos \theta_C)^2} = 6289s, \quad (8)$$

where the θ_C is the Cabibbo angle.

The Fermi reduced transition probability $B(F)$ is given by

$$B(F) \equiv \frac{g_V^2}{2J_i + 1} |M_F|^2, \quad (9)$$

where M_F is the Fermi matrix element.

The phase-space factor for β^+ -decay is given by

$$f_0^{(+)} = \int_1^{E_0} F_0(-Z_f, \epsilon) p \epsilon (E_0 - \epsilon)^2 d\epsilon, \quad (10)$$

where $F_0(-Z_f, \epsilon)$ is called the Fermi function and

$$\epsilon \equiv \frac{E_e}{m_e c^2}, E_0 \equiv \frac{E_i - E_f}{m_e c^2}, p \equiv \sqrt{\epsilon^2 - 1}, \quad (11)$$

where E_e is the total energy of the emitted positron and E_i and E_f are the energies of the initial and final nuclear states, respectively.

Following Ref. [31], the phase-space factor for the EC transition is given by

$$f_0^{(EC)} = 2\pi(\alpha Z_i)^3 (\epsilon_0 + E_0)^2, \quad (12)$$

where ϵ_0 is given by

$$\epsilon_0 \equiv 1 - \frac{1}{2}(\alpha Z_i)^2, \quad (13)$$

and α ($= \frac{1}{137}$) represents the fine-structure constant. The non-relativistic s -electron wave function are considered in Eq. 13, and this approximation not holds good for small decay energies, additional corrections arise from the screening of the nuclear charge by atomic electrons and from the finite nuclear size.

The experimental β -decay Q values are taken from [32].

Usually, ft values are large, expressed in terms of ‘log ft values’. The $\log ft \equiv \log_{10}(f_0 t_{1/2}[s])$.

The total half-life can be calculated with the help of the partial half-life (t_i) of the daughter states i using the following expression:

$$\frac{1}{t_{1/2}} = \left(\sum_i \frac{1}{t_i} \right). \quad (14)$$

The expression for the partial half-life of the allowed β -decay is taken from [31].

The branching ratio b_r is related to partial half-life t_i and the total half-life $t_{1/2}$ of the allowed β -decay as

$$t_i = \frac{t_{1/2}}{b_r}. \quad (15)$$

where t_i is the partial half-life and $t_{1/2}$ is the total half-life of the allowed β -decay.

2.2 The Q -value formalism

The theoretical β^+ -decay Q -values were obtained using following relation [33]

$$Q(\beta^+) = E_{g.s}^{parent} - E_{g.s}^{daughter} + \delta m, \quad (16)$$

where $E_{g.s}^{parent}$ and $E_{g.s}^{daughter}$ represent the ground state binding energies of parent and daughter nuclei, respectively, and $\delta m = (m_p - m_n - m_{e^+})c^2 = -1.802$ MeV.

The binding energy of the ground state is given by

$$E = E_{SM} + E_{core} + E_C, \quad (17)$$

where E_{SM} is the calculated binding energy using shell-model and E_{core} is the binding energy of the considered core in SM calculations, and E_C is the valence space Coulomb energy. In [34], the expression for E_C is given as

$$E_C = 0.700[Z(Z-1) - 0.76(Z(Z-1))^{2/3}]/R_C, \quad (18)$$

$$R_C = e^{1.5/A} A^{1/3} \left(0.946 - 0.573 \left(\frac{2T}{A} \right)^2 \right), \quad (19)$$

where T is the isospin of the nucleus.

2.3 Shell Model Hamiltonian, Model space and quenching factor

The β^+ -decay half-lives calculation has been performed for nuclei in sd model space using USDB [35] and SDNN [5] effective interactions. The NuShellX@MSU [36] shell model code has been used to diagonalize energy matrices. The USDB Hamiltonian is the mass-dependent version of USD [37,29] and the mass dependence of TBMEs have the form $[18/(16+n)]^{0.3}$, where the number of valence nucleons is represented by n . The single-particle energies for USDB Hamiltonian are taken to be 2.1117, -3.9257, and -3.2079 in MeV for the $d_{3/2}$, $d_{5/2}$ and $s_{1/2}$ orbits, respectively. The USDB interaction is characterized by 66 parametric values, viz., three bare single-particle energies and 33 and 30 TBMEs of $T = 0$ and 1, respectively. In the SDNN interaction, Hamiltonian [5], the USDB interaction was re-estimated for $N = Z$ nuclei using artificial neural networks.

The theoretical SM results of Gamow-Teller transition strengths are more significant than the experimental ones. Hence, we need a quenching factor (q) for this model space to better agreement between theoretical and experimental results. Using Eq. 3 - 5, we have calculated theoretical and experimental $R(GT)$ values for a particular model space by averaging all the ratios between the experimental and theoretical $R(GT)$ values we get quenching factor (q). The comparison between experimental and theoretical $R(GT)$ values are plotted in Fig. 1. To get experimental $R(GT)$ values, we took experimental $\log ft$ values, which are listed in Table 1. In Fig. 1, the slope of the straight line gives the average quenching factor. In the present work, we have obtained two different quenching factors for sd shell nuclei, $q = 0.794 \pm 0.05$ using USDB, and $q = 0.815 \pm 0.04$ using SDNN effective interactions.

3 Results and discussions

We have compared the experimental matrix elements $M(GT)$ of 116 pure Gamow-Teller decays with the theoretical shell-model results using USDB and SDNN interactions in Table 1. In most cases, the computed values are clearly systematically larger than the experimental ones. We have plotted the experimental values versus the theoretical ones for $R(GT)$ in Fig. 1. Each Gamow-Teller transition is represented by a point in Fig. 1. The points follow a straight line whose slope gives the average quenching factor, $q = 0.794 \pm 0.05$ for USDB interaction and $q = 0.815 \pm 0.04$ for SDNN interaction. The eight individual Gamow-Teller transition strengths of ^{33}Ar have been used to calculate the quenching factor 0.700 ± 0.002 for sd space using USD interaction in [38]. In [14], the quenching factor 0.6 is reported for sd space using USD interaction. In the previous work by Wildenthal *et al.* [39], where $q = 0.77 \pm 0.02$ has been reported for selected sd shell nuclei. The calculated quenching factor in the present work is slightly greater than the previous works [38], [14], [39]. Our calculated average quenching factors are more closer to unity.

Table 1. Listed the experimental and theoretical $M(GT)$ matrix elements; $I_\beta + I_\epsilon$ are the branching ratios; J_n^π and T_n^π are the spin-parity and isospin of the final states, respectively.

Process	$2J_n^\pi, 2T_n^\pi$	$Q(\text{MeV})$	$I_\beta + I_\epsilon$ (%)	$\log ft$	$M(GT)$			W
					EXPT.	USDB	SDNN	
$^{18}\text{Ne}(\beta^+)^{18}\text{F}$	$2_1^+, 0$	4445.7(47)	92.08	3.091	1.778	2.279	2.279	3.111
	$2_2^+, 0$	2744.8	0.188	4.47	0.363	0.269	0.266	
$^{20}\text{Na}(\beta^+)^{20}\text{Ne}$	$6_1^+, 0$	4403	0.028	5.77	0.182	0.436	0.454	6.956
	$6_2^+, 0$	3002	0.117	4.36	0.923	0.709	0.649	
$^{21}\text{Na}(\beta^+)^{21}\text{Ne}$	$5_1^+, 1$	3196.4	5.067	4.596	0.629	0.802	0.779	4.399
	$1_1^+, 1$	753	–	4.61	0.619	0.653	0.643	
$^{22}\text{Na}(\beta^+)^{22}\text{Ne}$	$4_1^+, 2$	1568.67	99.94	7.41	0.033	0.053	0.065	6.956
$^{21}\text{Mg}(\beta^+)^{21}\text{Na}$	$3_1^+, 1$	13098(16)	16	5.26	0.359	0.295	0.292	9.333
	$7_2^+, 1$	11382	10.9	5.11	0.426	0.761	0.736	
$^{22}\text{Mg}(\beta^+)^{22}\text{Na}$	$2_1^+, 0$	4198.55	41.32	3.64	0.945	1.182	1.189	3.111
	$2_2^+, 0$	2844.7	5.448	3.46	1.163	1.466	1.491	
$^{23}\text{Mg}(\beta^+)^{23}\text{Na}$	$5_1^+, 1$	3615.97	7.849	4.434	0.758	0.966	0.952	4.399
	$1_1^+, 1$	1665.27	0.006	4.97	0.409	0.689	0.673	
$^{22}\text{Al}(\beta^+)^{22}\text{Mg}$	$6_1^+, 2$	13149.2	5.9	5.56	0.311	0.538	0.520	13.198
	$6_2^+, 2$	11736	3	5.6	0.297	0.153	0.170	
$^{22}\text{Al}(\beta^+)^{22}\text{Mg}$	$10_1^+, 2$	11469	18.5	4.75	0.790	0.991	0.979	
$^{23}\text{Al}(\beta^+)^{23}\text{Mg}$	$3_1^+, 1$	12221.6(4)	36.3	5.3	0.342	0.281	0.267	9.333
$^{25}\text{Al}(\beta^+)^{25}\text{Mg}$	$3_2^+, 1$	3301.95	0.047	6.2	0.121	0.173	0.182	5.388
	$7_1^+, 1$	2664.93	0.783	4.36	1.011	1.167	1.170	
$^{25}\text{Si}(\beta^+)^{25}\text{Al}$	$3_1^+, 1$	11795	26	5.05	0.457	0.563	0.580	9.333
	$3_2^+, 1$	10068	4.8	5.42	0.298	0.542	0.593	
	$3_3^+, 1$	8551	2.99	5.25	0.363	0.368	0.357	
	$3_4^+, 1$	6570	0.32	5.6	0.242	0.416	0.412	
$^{26}\text{Si}(\beta^+)^{26}\text{Al}$	$3_5^+, 1$	5633	3.7	4.16	1.272	0.357	0.357	
	$2_1^+, 0$	4011.4	21.92	3.54	1.060	1.302	1.258	3.111
$^{26}\text{Si}(\beta^+)^{26}\text{Al}$	$2_2^+, 0$	3218.52	2.72	3.86	0.734	0.978	1.040	
	$2_3^+, 0$	1345.33	$\leq 5 \cdot 10^{-4}$	4.2	0.496	0.514	0.576	
$^{27}\text{Si}(\beta^+)^{27}\text{Al}$	$3_1^+, 1$	3797.82	0.006	7.23	0.037	0.228	0.322	5.388
	$7_1^+, 1$	2600.25	0.179	4.69	0.691	0.864	0.866	
$^{26}\text{P}(\beta^+)^{26}\text{Si}$	$3_2^+, 1$	1830.18	0.025	4.34	1.034	1.427	1.355	
	$4_1^+, 2$	16460.73	44	4.9	0.586	0.854	0.835	11.640
	$4_2^+, 2$	15741.69	3.3	5.9	0.185	0.099	0.075	
	$8_1^+, 2$	14415.8	1.68	6.0	0.165	0.187	0.169	
$^{26}\text{P}(\beta^+)^{26}\text{Si}$	$4_3^+, 2$	14118.82	1.78	5.9	0.294	0.442	0.429	
	$4_4^+, 2$	11963	0.78	5.9	0.415	0.037	0.026	
	$4_1^+, 0$	12556.07	69.1	4.851	0.620	0.750	0.720	8.231
	$8_1^+, 0$	9727.57	1.29	5.99	0.167	0.298	0.305	
$^{29}\text{P}(\beta^+)^{29}\text{Si}$	$3_1^+, 1$	3669.11	1.263	4.806	0.349	0.256	0.291	3.111
	$3_2^+, 1$	2516.52	0.45	4.172	0.724	1.053	1.046	
$^{30}\text{P}(\beta^+)^{30}\text{Si}$	$0_1^+, 2$	4232.4(3)	99.94	4.839	0.412	0.473	0.444	6.956
	$4_1^+, 2$	1997.08	0.052	5.884	0.124	0.169	0.210	
	$4_2^+, 2$	733.85	0.002	5.26	0.254	0.372	0.331	
	$0_2^+, 2$	462.88	0.003	4.48	0.622	0.781	0.794	3.111
$^{29}\text{S}(\beta^+)^{29}\text{P}$	$3_1^+, 1$	12411.45	27	5.06	0.451	0.735	0.738	9.333
	$3_2^+, 1$	11372.3	20.7	4.98	0.495	0.467	0.481	
$^{29}\text{S}(\beta^+)^{29}\text{P}$	$7_1^+, 1$	9714.5	3.9	5.03	0.467	0.643	0.713	
$^{30}\text{S}(\beta^+)^{30}\text{P}$	$2_1^+, 0$	6138(3)	21.3	4.322	0.431	0.472	0.444	3.111
	$2_2^+, 0$	5429.3	0.29	5.89	0.071	0.291	0.321	
	$2_3^+, 0$	3118.8	2.283	3.549	1.050	1.235	1.313	
$^{31}\text{Cl}(\beta^+)^{31}\text{S}$	$1_1^+, 1$	12008(3)	7.0	5.6	0.198	0.274	0.279	7.620
	$5_1^+, 1$	9773.94	38	4.37	0.816	1.139	1.133	

Table 1. Continuation.

Process	$2J_n^\pi, 2T_n^\pi$	$Q(\text{MeV})$	$I_\beta + I_\epsilon$ (%)	$\log ft$	$M(GT)$			W
					EXPT.	USDB	SDNN	
$^{33}\text{Cl}(\beta^+)^{33}\text{S}$	$1_2^+, 1$	8931.56	2.54	5.33	0.270	0.289	0.258	4.399
	$5_2^+, 1$	8724.24	4.46	5.03	0.382	0.487	0.485	
	$1_1^+, 1$	4741.69	0.48	5.65	0.187	0.229	0.238	
	$5_1^+, 1$	3615.99	0.461	4.97	0.409	0.367	0.392	
	$5_2^+, 1$	2715.09	0.436	4.18	1.015	1.125	1.179	
	$5_3^+, 1$	1750.29	$\leq 7 \cdot 10^{-4}$	6.4	0.079	0.521	0.509	
$^{34}\text{Cl}(\beta^+)^{34}\text{S}$	$1_2^+, 1$	1529.39	$1 \cdot 10^{-4}$	6.2	0.099	0.312	0.314	6.956
	$1_3^+, 1$	1207.09	$\leq 4 \cdot 10^{-4}$	5.7	0.176	0.505	0.510	
	$4_1^+, 2$	3364.07	28.52	5.982	0.169	0.242	0.196	
	$4_2^+, 2$	2187.42	26.42	4.823	0.641	0.910	0.926	
	$4_3^+, 2$	1376.82	0.457	5.081	0.476	0.711	0.736	
	$8_1^+, 2$	802.65	0.033	5.44	0.315	0.286	0.306	
$^{34}\text{Cl}(\beta^+)^{34}\text{S}$	$2_1^+, 2$	11134.7	≤ 7	≥ 5.1	0.155	0.082	0.085	9.333
$^{32}\text{Ar}(\beta^+)^{32}\text{Cl}$	$2_2^+, 2$	9966.15	57	3.94	0.669	0.909	0.907	4.399
	$2_3^+, 2$	8924.5	0.35	5.9	0.070	0.215	0.214	
	$2_4^+, 2$	7362.7	3.681	4.424	0.383	0.388	0.376	
	$2_5^+, 2$	6967.7	0.9	4.9	0.222	0.184	0.174	
	$2_6^+, 2$	6695.7	0.117	5.7	0.088	0.832	0.859	
	$2_7^+, 2$	6338.7	0.053	5.91	0.069	0.324	0.237	
	$2_8^+, 2$	5832.7	0.115	5.371	0.129	0.417	0.461	
	$2_9^+, 2$	5439.7	0.231	4.9	0.222	0.371	0.360	
	$2_{10}^+, 2$	5071.7	0.146	4.92	0.217	0.541	0.521	
	$2_{11}^+, 2$	4606.7	0.049	5.16	0.164	0.412	0.420	
	$2_{12}^+, 2$	4396.7	0.127	4.62	0.306	1.207	1.750	
	$2_{13}^+, 2$	3804.7	0.125	4.26	0.463	1.157	0.202	
	$2_{14}^+, 2$	3526.7	0.007	5.4	0.125	0.666	0.774	
	$2_{15}^+, 2$	3273.7	0.046	4.49	0.355	0.330	0.119	
$^{33}\text{Ar}(\beta^+)^{33}\text{Cl}$	$3_1^+, 1$	11619.1(6)	18.7	5.022	0.272	0.324	0.335	
	$3_2^+, 1$	9266.8	1.7	5.54	0.150	0.361	0.351	3.111
	$3_3^+, 1$	7648.1	0.382	5.744	0.119	0.166	0.183	
	$3_4^+, 1$	7506.1	0.453	5.626	0.136	0.388	0.378	
$^{34}\text{Ar}(\beta^+)^{34}\text{Cl}$	$2_1^+, 0$	5601.03	0.91	5.31	0.138	0.084	0.077	
	$2_2^+, 0$	5396.03	2.492	4.78	0.254	0.489	0.481	4.399
	$2_3^+, 0$	3482.33	0.864	4.12	0.544	0.396	0.482	
	$2_4^+, 0$	2932.63	1.29	3.458	1.165	1.226	1.245	
$^{35}\text{Ar}(\beta^+)^{35}\text{Cl}$	$1_1^+, 1$	4746.88	1.232	5.091	0.356	0.430	0.438	4.399
	$5_1^+, 1$	4202.99	0.248	5.475	0.229	0.410	0.403	
	$5_2^+, 1$	2963.8	0.088	4.973	0.400	0.528	0.326	
$^{35}\text{K}(\beta^+)^{35}\text{Ar}$	$1_2^+, 1$	1998.4	0.007	4.81	0.491	0.599	0.589	7.620
	$5_1^+, 1$	10123.8	11.901	4.91	0.438	0.636	0.623	
	$5_2^+, 1$	8891.7	26	4.27	0.915	1.111	1.129	4.399
$^{35}\text{K}(\beta^+)^{35}\text{Ar}$	$1_1^+, 1$	7168.6	2.1	4.85	0.469	0.574	0.559	
$^{37}\text{K}(\beta^+)^{37}\text{Ar}$	$1_1^+, 1$	4737.66	0.004	7.38	0.025	0.069	0.072	4.399
	$5_1^+, 1$	3351.38	2.067	3.785	1.600	1.765	1.936	
	$5_2^+, 1$	2977.68	0.003	6.34	0.084	1.248	1.017	
$^{38}\text{K}(\beta^+)^{38}\text{Ar}$	$4_1^+, 2$	3746.47	99.84	4.975	0.538	0.922	0.922	6.956
	$4_2^+, 2$	1978.27	0.151	5.88	0.190	3.771	0.154	4.399
$^{36}\text{Ca}(\beta^+)^{36}\text{K}$	$2_1^+, 2$	9853.6	14.302	4.519	0.344	0.751	0.733	
	$2_2^+, 2$	9347.4	31.007	4.06	0.583	0.748	0.789	
	$2_3^+, 2$	7609	10.304	4.06	0.583	0.297	0.278	
	$2_4^+, 2$	6516	2.602	4.29	0.447	0.725	0.717	
	$2_5^+, 2$	6308	1.2	4.55	0.332	0.363	0.393	

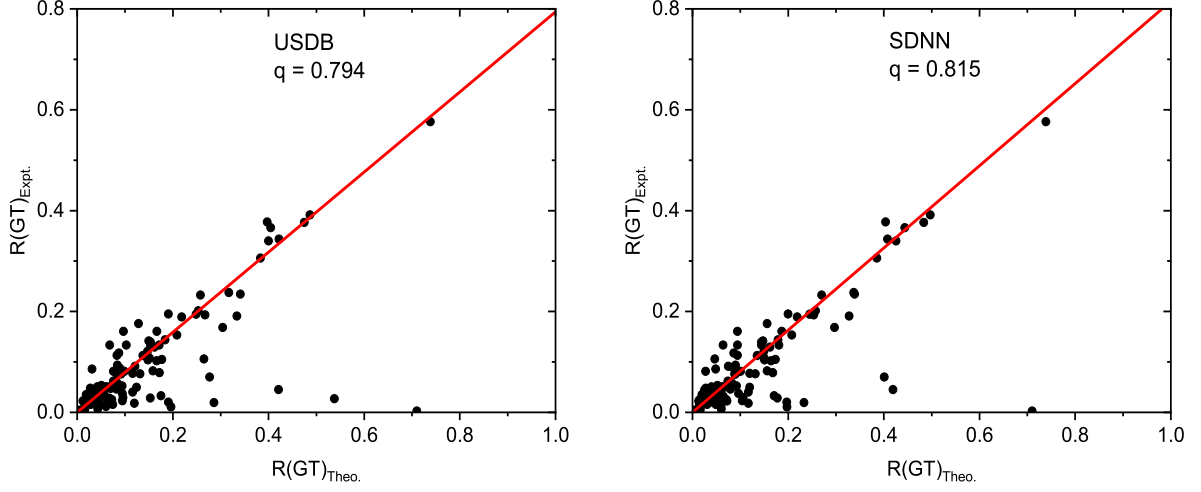


Fig. 1. The experimental versus theoretical matrix element $R(GT)$ values. SM calculations are based on the “free-nucleon” Gamow-Teller operator. Each transitions are represented by a point in the graph. The theoretical and experimental values are taken on the x and y axes, respectively.

Table 1. Continuation.

Process	$2J_n^\pi, 2T_n^\pi$	$Q(\text{MeV})$	$I_\beta + I_\epsilon$		$M(GT)$			W
			(%)	$\log ft$	EXPT.	USDB	SDNN	
$^{37}\text{Ca}(\beta^+)^{37}\text{K}$	$2_6^+, 2$	5040	2.204	3.73	0.852	0.831	0.871	7.620
	$2_7^+, 2$	4179	0.502	3.9	0.701	0.421	0.410	
	$2_1^+, 1$	10293.6	2.14	5.69	0.089	0.453	0.452	
	$5_1^+, 1$	8914	7.9	4.79	0.251	1.325	1.290	
$^{38}\text{Ca}(\beta^+)^{38}\text{K}$	$5_2^+, 1$	8425	4.5	4.9	0.222	0.201	0.370	3.111
	$2_1^+, 0$	6283.7	2.842	4.8	0.249	0.277	0.276	
	$2_2^+, 0$	5044.5	19.478	3.426	1.209	1.502	1.534	
	$2_3^+, 0$	3401.1	0.343	4.16	0.519	0.938	0.916	
	$2_4^+, 0$	2886.46	0.025	4.8	0.249	0.010	0.010	
	$2_5^+, 0$	2765.9	0.112	4.05	0.590	1.030	1.011	
$^{39}\text{Ca}(\beta^+)^{39}\text{K}$	$2_6^+, 0$	2567.3	0.004	5.3	0.140	1.299	1.293	4.399
	$1_1^+, 1$	4002.16	0.0025	7.020	0.019	0.006	0.020	

Table 2. Listed the theoretical phase space factors for β^+/EC decay (considered only those nuclei in which the EC phase space factors are significant); $\log(f_0^{(+)} + f_0^{(EC)})$ values; the experimental Q values taken from [32].

$^A Z_i(J^\pi)$	$^A Z_f(J^\pi)$	$Q^{(EXPT.)}$ (MeV)	$f_0^{(+)}$	$f_0^{(EC)}$	$\log(f_0^{(+)} + f_0^{(EC)})$
$^{22}\text{Na}(3^+)$	$^{22}\text{Ne}(2_1^+)$	1.568	0.2806	0.0306	-0.5072
$^{23}\text{Mg}(3/2^+)$	$^{23}\text{Na}(3/2_1^+)$	4.056	376.172	0.2658	2.5757
	$^{23}\text{Na}(5/2_1^+)$	3.615	186.951	0.2111	2.272
$^{29}\text{P}(1/2^+)$	$^{23}\text{Na}(1/2_1^+)$	1.665	0.5233	0.0497	-0.2418
	$^{29}\text{Si}(1/2_1^+)$	4.942	1125.19	0.7704	3.0515
	$^{29}\text{Si}(3/2_1^+)$	3.669	192.259	0.4244	2.2848
$^{30}\text{P}(1^+)$	$^{29}\text{Si}(3/2_2^+)$	2.516	15.9367	0.1994	1.2078
	$^{30}\text{Si}(0_1^+)$	4.232	455.214	0.5648	2.6587
$^{34}\text{Cl}(3^+)$	$^{30}\text{Si}(2_1^+)$	1.997	2.642	0.1256	0.4421
	$^{34}\text{S}(2_1^+)$	3.364	107.342	0.5191	2.0328
	$^{34}\text{S}(2_2^+)$	2.187	5.2964	0.2191	0.7416
$^{38}\text{K}(3^+)$	$^{34}\text{S}(2_3^+)$	1.376	0.0396	0.0865	-0.8993
	$^{38}\text{Ar}(2_1^+)$	3.746	201.575	0.8983	2.3064
	$^{38}\text{Ar}(2_2^+)$	1.978	2.1988	0.2499	0.3889
	$^{38}\text{Ar}(2_3^+)$	1.348	2.6119	0.1158	0.4358

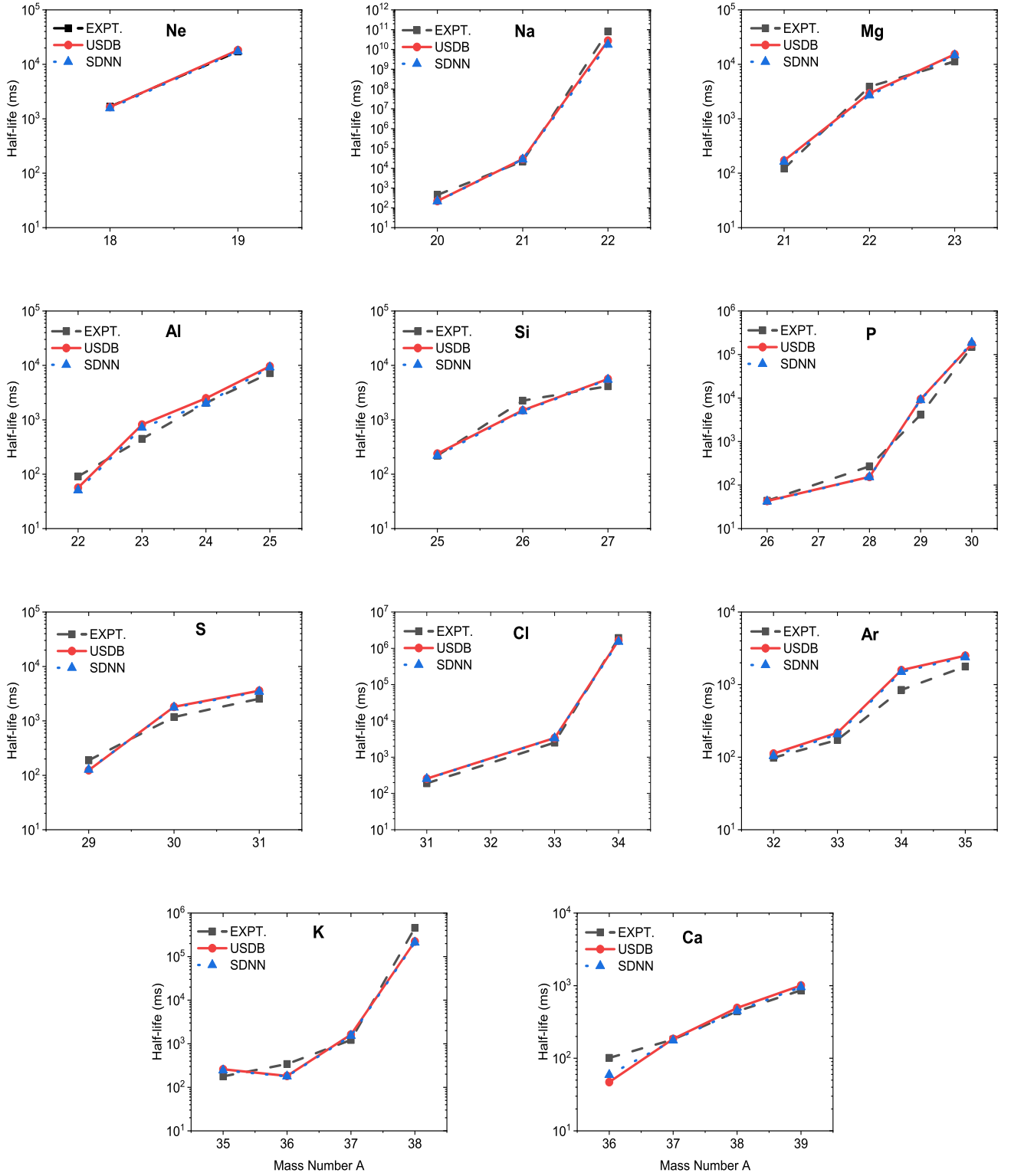


Fig. 2. The theoretical and experimental β^+/EC - decay half-life versus mass number A of the concerned *sd* shell nuclei.

Table 3. The theoretical $\log ft$ values, excitation energies, and branching percentages of β^+ /EC -decays of the concerned nuclei are compared with the experimental data; References of the experimental data are given in the last column.

${}^AZ_i(J^\pi)$	${}^AZ_f(J^\pi)$	Ex. energy (keV)			$\log ft$ value			Branching (%)			Ref.
		USDB	SDNN	EXPT.	USDB	SDNN	EXPT.	USDB	SDNN	EXPT.	
${}^{18}\text{Ne}(0^+)$	${}^{18}\text{F}(1^+)$	0	0	0	3.076	3.053	3.091	95.05	95.05	92.1	[7]
${}^{19}\text{Ne}(1/2^+)$	${}^{19}\text{F}(1/2^+)$	0	0	0	3.218	3.201	3.232	99.99	99.99	99.88	[41]
${}^{20}\text{Na}(2^+)$	${}^{19}\text{F}(3/2^+)$	1.770	1.789	1.554	7.791	7.769	5.71	$4 \cdot 10^{-6}$	$4 \cdot 10^{-6}$	0.002	[32]
	${}^{20}\text{Ne}(2^+)$	1.747	1.810	1.633	5.018	5.008	4.99	70.31	70.04	79.44	
		7.543	7.542	7.421	4.310	4.294	4.2	20.71	21.86	15.96	
		9.958	10.110	7.833	4.704	4.683	5.48	1.19	1.11	0.58	
		10.493	10.638	9.483	4.174	4.217	5.08	2.31	1.86	0.24	
		10.787	10.953	10.274	3.972	3.921	3.48	2.63	2.55	2.87	
		12.273	12.315	10.941	5.800	5.551	5.3	0.004	0.007	0.01	
		13.267	13.322	11.116	5.705	5.619	5.26	$5 \cdot 10^{-4}$	$6 \cdot 10^{-4}$	0.01	
		13.827	13.878	11.856	5.289	5.349	4.99	$1 \cdot 10^{-4}$	$1 \cdot 10^{-4}$	0.0016	
		${}^{20}\text{Ne}(3^+)$	10.485	10.531	9.873	5.210	5.349	5.77	0.21	0.24	
		10.554	10.692	10.884	4.789	4.843	4.36	0.52	0.41	0.11	
	${}^{20}\text{Ne}(1^+)$	11.166	12.754	11.262	3.871	3.850	3.72	2.07	1.88	0.2	
${}^{21}\text{Na}(3/2^+)$	${}^{21}\text{Ne}(3/2^+)$	0	0	0	3.624	3.617	3.608	91.81	90.92	94.93	[6]
	${}^{21}\text{Ne}(5/2^+)$	0.266	0.172	0.350	4.585	4.587	4.596	8.81	9.07	5.06	
	${}^{21}\text{Ne}(1/2^+)$	2.859	2.679	2.794	4.764	4.754	4.61	$3 \cdot 10^{-4}$	$5 \cdot 10^{-4}$	-	
${}^{22}\text{Na}(3^+)$	${}^{22}\text{Ne}(2^+)$	1.363	1.424	1.274	7.189	6.991	7.41	100	100	89.9	[42]
${}^{21}\text{Mg}(5/2^+)$	${}^{21}\text{Na}(3/2^+)$	0	0	0	5.630	5.616	5.26	9.62	9.49	16	[9]
	${}^{21}\text{Na}(5/2^+)$	0.266	0.172	0.331	4.787	4.777	4.79	60.19	61.21	41	
	${}^{21}\text{Na}(7/2^+)$	1.757	1.691	1.716	4.806	4.812	5.11	30.18	29.28	10.9	
${}^{22}\text{Mg}(0^+)$	${}^{22}\text{Na}(1^+)$	0.338	0.715	0.583	3.646	3.618	3.64	66.94	87.88	41.3	[8]
		2.041	1.871	1.936	3.459	3.422	3.46	7.03	12.11	5.44	
${}^{23}\text{Mg}(3/2^+)$	${}^{23}\text{Na}(3/2^+)$	0	0	0	3.694	3.692	3.667	88.14	86.73	92.14	[11]
	${}^{23}\text{Na}(5/2^+)$	0.399	0.332	0.440	4.423	4.413	4.434	11.08	13.18	7.84	
	${}^{23}\text{Na}(1/2^+)$	2.173	2.062	2.390	4.717	4.714	4.97	0.028	0.08	0.006	
${}^{22}\text{Al}((4)^+)$	${}^{22}\text{Mg}(4^+)$	3.357	3.385	5.293	6.888	6.769	4.87	49.22	50.91	31	[12]
		5.367	5.276	6.221	4.807	4.775	5.33	4.28	4.18	7.4	
	${}^{22}\text{Mg}(3^+)$	5.461	5.506	5.451	5.283	5.290	5.56	15.94	14.48	5.9	
		6.513	6.535	6.865	6.376	6.264	5.6	0.91	0.91	3	
	${}^{22}\text{Mg}(5^+)$	7.294	7.232	7.132	4.753	4.741	4.75	28.90	28.42	18.5	
${}^{23}\text{Al}(5/2^+)$	${}^{23}\text{Mg}(3/2^+)$	0	0	0	5.671	5.693	5.3	29.42	23.82	36.3	[43]
	${}^{23}\text{Mg}(5/2^+)$	0.399	0.332	0.451	5.630	5.559	5.36	27.21	28.08	26.2	
		3.750	3.685	7.803	7.490	7.167	3.31	0.07	0.11	13.4	
		5.422	5.319	8.164	5.667	5.675	4.77	1.28	1.17	0.28	
	${}^{23}\text{Mg}(7/2^+)$	2.169	2.105	2.051	6.645	6.538	5.67	1.09	1.27	5.91	
	4.662	4.554	7.848	6.212	6.250	5.3	0.65	0.55	0.11		
${}^{24}\text{Al}(4^+)$	${}^{24}\text{Mg}(4^+)$	4.372	4.336	4.122	5.899	5.805	6.13	100	100	7.7	[13]
${}^{25}\text{Al}(5/2^+)$	${}^{25}\text{Mg}(5/2^+)$	0	0	0	3.588	3.582	3.57	99.25	99.22	99.25	[6]
	${}^{25}\text{Mg}(3/2^+)$	1.097	1.122	0.974	6.092	6.028	6.2	0.06	0.06	0.07	
	${}^{25}\text{Mg}(7/2^+)$	1.720	1.715	1.611	4.436	4.411	4.36	0.67	0.68	0.70	
${}^{25}\text{Si}(5/2^+)$	${}^{25}\text{Al}(5/2^+)$	0	0	0	5.277	5.189	5.24	28.99	28.60	25	[14]
		1.995	1.993	3.844	6.148	6.036	6.21	1.60	1.67	0.4	
		3.908	4.033	4.582	6.791	6.769	5.11	0.12	0.196	3.2	
		4.740	4.749	5.802	5.090	5.057	5	3.79	3.27	1.7	
		5.799	5.817	6.620	5.805	4.290	5.7	0.33	0.005	0.16	
	${}^{25}\text{Al}(3/2^+)$	1.097	1.122	0.945	5.069	5.020	5.05	29.22	26.05	26	
		2.811	2.879	2.672	5.102	5.000	5.42	11.68	11.48	4.8	
		4.332	4.369	4.189	5.437	5.440	5.25	1.59	1.74	2.99	
		5.788	5.781	6.170	5.330	5.317	5.6	1.01	0.85	0.32	
		6.346	6.334	7.107	5.465	5.440	4.16	0.40	0.47	3.7	
${}^{26}\text{Si}(0^+)$	${}^{25}\text{Al}(7/2^+)$	1.720	1.715	1.613	5.156	5.151	5.16	17.89	14.64	15	[6]
	${}^{26}\text{Al}(1^+)$	0.806	1.088	1.057	3.562	3.569	3.54	55.71	52.91	21.9	
		1.589	1.862	1.850	3.811	3.735	3.86	11.87	13.80	2.72	
		1.880	2.141	2.071	5.443	5.379	4.63	0.18	0.21	0.28	
		2.524	2.749	2.740	4.369	4.248	4.54	0.73	1.03	0.06	
	3.428	3.674	3.723	5.053	4.706	>4.2	0.018	0.043	<0.001		
${}^{27}\text{Si}(5/2^+)$	${}^{27}\text{Al}(5/2^+)$	0	0	0	3.631	3.632	>3.6	99.52	99.33	<99.71	[15]
		2.699	2.770	2.734	4.797	4.777	5	0.04	0.03	0.02	
	${}^{27}\text{Al}(3/2^+)$	1.063	1.095	1.014	5.852	5.531	7.23	0.18	0.34	0.006	
		2.841	2.810	2.982	4.260	4.283	4.34	0.07	0.08	0.02	
	${}^{27}\text{Al}(7/2^+)$	2.328	2.280	2.212	4.697	4.672	4.69	0.17	0.2	0.18	
${}^{26}\text{P}(3^+)$	${}^{26}\text{Si}(2^+)$	1.897	1.982	1.797	4.773	4.771	4.9	60.67	59.66	44	[14]

Table 3. *Continuation.*

${}^AZ_i(J^\pi)$	${}^AZ_f(J^\pi)$	Ex. energy (keV)			logft value			Branching (%)			Ref.	
		USDB	SDNN	EXPT.	USDB	SDNN	EXPT.	USDB	SDNN	EXPT.		
		3.007	3.102	2.786	6.645	6.866	5.9	0.6	0.33	3.3		
		4.449	4.550	4.139	5.607	5.523	5.9	3.92	4.49	1.78		
		4.882	4.995	6.295	5.346	5.349	5.9	6.94	5.68	0.78		
		5.385	5.615	6.384	7.490	7.769	5.5	0.04	0.01	1.7		
		6.676	6.799	7.501	6.075	6.145	5.2	0.53	0.43	2.4		
	${}^{26}\text{Si}(3^+)$	3.882	3.889	3.756	6.129	6.013	5.8	1.40	1.84	2.68		
		4.317	4.451	4.186	5.133	5.119	5.7	11.88	11.78	2.91		
		6.179	6.283	5.928	4.791	4.717	4.6	12.71	14.63	18		
	${}^{26}\text{Si}(4^+)$	4.365	4.346	3.842	6.092	6.156	6	1.29	1.13	1.68		
	${}^{28}\text{P}(3^+)$	${}^{28}\text{Si}(2^+)$	1.932	2.004	1.779	4.886	4.899	4.851	73.18	70.01	69.1	[44]
		${}^{28}\text{Si}(4^+)$	4.607	4.591	4.617	5.688	5.645	5.99	3.93	4.44	1.29	
		${}^{28}\text{Si}(3^+)$	6.330	6.194	6.276	4.558	4.551	4.788	22.88	25.54	7.6	
	${}^{29}\text{P}(1/2^+)$	${}^{29}\text{Si}(1/2^+)$	0	0	0	3.706	3.702	3.681	96.74	96.62	98.29	[6]
		${}^{29}\text{Si}(3/2^+)$	1.285	1.266	1.273	5.277	5.143	4.806	0.25	0.33	1.26	
			2.525	2.659	2.425	4.047	4.030	4.172	3.00	3.04	0.45	
	${}^{30}\text{P}(1^+)$	${}^{30}\text{Si}(0^+)$	0	0	0	4.919	4.950	4.839	99.92	99.81	99.93	[6]
			3.912	3.963	3.787	5.128	5.205	4.48	0.002	0.002	0.003	
		${}^{30}\text{Si}(2^+)$	2.266	2.296	2.235	5.814	5.601	5.884	0.06	0.1	0.05	
			3.506	3.590	3.498	6.260	6.371	5.26	0.002	0.002	0.001	
		${}^{30}\text{Si}(1^+)$	4.065	4.151	3.769	4.483	4.447	5.79	$1 \cdot 10^{-4}$	$1 \cdot 10^{-5}$	$1 \cdot 10^{-4}$	
	${}^{29}\text{S}((5/2)^+)$	${}^{29}\text{P}(3/2^+)$	1.285	1.266	1.383	4.837	4.811	5.06	52.98	54.15	27	[45]
			2.525	2.659	2.422	5.230	5.182	4.98	13.10	13.21	20.7	
			6.047	6.091	9.389	6.376	6.468	4.4	0.16	0.123	0.43	
		${}^{29}\text{P}(5/2^+)$	2.063	2.068	1.953	5.899	5.665	5.73	3.39	5.60	4.5	
			3.356	3.359	3.105	6.043	5.976	6.2	1.47	1.57	0.9	
			4.900	4.831	4.954	4.628	4.650	4.639	17.41	16.37	11.9	
		${}^{29}\text{P}(7/2^+)$	4.222	4.188	4.080	7.791	7.070	>6.2	0.017	0.085	< 0.5	
			5.122	5.156	5.293	4.952	4.841	5.03	7.33	8.88	3.9	
	${}^{30}\text{S}(0^+)$	${}^{30}\text{P}(1^+)$	0	0	0	4.443	4.473	4.322	25.26	22.88	21.3	[6]
			0.647	0.660	0.708	4.862	4.756	5.89	5.14	6.31	0.29	
			3.138	3.285	3.019	3.608	3.531	3.549	2.44	2.03	2.28	
	${}^{31}\text{S}(1/2^+)$	${}^{31}\text{P}(1/2^+)$	0	0	0	3.687	3.688	3.678	98.36	98.06	98.85	[6]
			3.236	3.261	3.134	4.917	4.851	4.76	0.02	0.02	0.03	
		${}^{31}\text{P}(3/2^+)$	1.173	1.133	1.266	5.005	4.939	4.96	1.60	1.90	1.1	
			3.625	3.772	3.506	4.371	4.359	4.57	0.01	0.007	0.01	
	${}^{31}\text{Cl}(3/2^+)$	${}^{31}\text{S}(1/2^+)$	0	0	0	5.517	5.481	5.6	10.74	11.02	7	[18]
			3.237	3.261	3.076	5.471	5.546	5.33	2.25	1.76	2.54	
		${}^{31}\text{S}(3/2^+)$	1.174	1.133	1.248	5.285	5.235	6.1	10.64	11.54	1.1	
			3.626	3.772	3.434	6.449	6.145	5.84	0.18	0.31	0.64	
			4.375	4.457	4.207	4.843	5.756	4.81	4.5	3.52	4.1	
		${}^{31}\text{S}(5/2^+)$	2.306	2.275	2.234	4.280	4.263	4.37	59.97	60.04	38	
			3.313	3.280	3.283	5.018	4.999	5.03	6.09	6.14	4.46	
	${}^{33}\text{Cl}(3/2^+)$	${}^{33}\text{S}(3/2^+)$	0	0	0	3.732	3.730	3.747	95.48	98.30	98.58	[6]
			2.241	2.220	2.312	5.823	5.756	5.82	0.05	0.06	0.04	
			3.585	3.615	3.935	5.972	6.013	>6.3	0.001	$8 \cdot 10^{-4}$	< $1 \cdot 10^{-4}$	
		${}^{33}\text{S}(1/2^+)$	0.852	0.831	0.840	5.674	5.616	5.65	0.63	0.7	0.48	
			3.943	3.996	4.053	5.404	5.376	6.2	$7 \cdot 10^{-4}$	$6 \cdot 10^{-4}$	$1 \cdot 10^{-4}$	
			4.277	4.299	4.375	4.987	4.955	5.7	$4 \cdot 10^{-4}$	$4 \cdot 10^{-4}$	< $1 \cdot 10^{-4}$	
		${}^{33}\text{S}(5/2^+)$	1.923	1.889	1.966	4.264	5.183	4.97	0.35	0.42	0.46	
			2.949	2.906	2.867	4.291	4.228	4.18	0.39	0.48	0.43	
			3.842	3.856	3.832	4.959	4.958	>6.4	0.003	0.003	<0.0001	
	${}^{34}\text{Cl}(3^+)$	${}^{34}\text{S}(2^+)$	2.131	2.135	2.127	5.867	6.028	5.982	16.78	26.34	28.52	[46]
			3.123	3.133	3.304	4.719	4.680	4.823	23.12	23.33	26.42	
			4.126	4.186	4.114	4.933	4.880	5.081	0.37	0.38	0.45	
		${}^{34}\text{S}(4^+)$	4.836	4.790	4.688	5.723	5.642	5.44	39.99	46.718	–	
		${}^{34}\text{S}(3^+)$	4.702	4.682	4.876	5.264	5.187	5.18	10.17	12.78	–	
	${}^{32}\text{Ar}(0^+)$	${}^{32}\text{Cl}(1^+)$	0	0	0	5.959	5.905	>5.1	1.13	1.19	<7	[16]
			1.119	1.082	1.168	3.874	3.854	3.94	78.51	78.39	57	
			1.981	1.958	2.210	5.125	5.110	5.9	2.73	2.67	0.35	
			2.875	2.861	3.772	4.614	4.618	4.424	5.11	4.77	3.68	
			3.806	3.825	4.167	5.262	5.289	4.9	0.6	0.52	0.9	
	${}^{33}\text{Ar}(1/2^+)$	${}^{33}\text{Cl}(3/2^+)$	0	0	0	5.071	5.020	5.022	21.19	22.76	18.7	[38]
			2.241	2.220	2.352	4.977	4.980	5.54	8.15	8.50	1.7	
			3.585	3.615	3.971	5.651	5.546	5.744	0.94	0.79	0.38	

Table 3. *Continuation.*

${}^A Z_i(J^\pi)$	${}^A Z_f(J^\pi)$	Ex. energy (keV)			log ft value			Branching (%)			Ref.	
		USDB	SDNN	EXPT.	USDB	SDNN	EXPT.	USDB	SDNN	EXPT.		
${}^{33}\text{Cl}(1/2^+)$		4.355	4.379	4.113	4.916	4.915	5.626	2.47	2.32	0.45		
		0.852	0.831	0.810	4.459	4.452	4.516	56.99	58.09	41		
		3.943	3.996	4.441	6.615	7.292	4.8	0.06	0.01	2.37		
		4.277	4.299	5.548	4.570	4.538	3.284	5.8	5.87	31		
		5.217	5.220	5.732	4.521	4.514	5.92	3.07	2.92	0.06		
${}^{34}\text{Ar}(0^+)$	${}^{34}\text{Cl}(1^+)$	0.325	0.361	0.460	5.940	5.991	5.31	0.63	0.53	0.91	[17]	
		0.512	0.543	0.665	4.413	4.405	4.78	17.64	17.24	2.49		
		2.372	2.420	2.579	4.596	4.403	4.12	1.30	1.88	0.86		
		3.031	3.069	3.129	3.615	3.578	3.458	4.23	4.12	1.29		
${}^{35}\text{Ar}(3/2^+)$	${}^{35}\text{Cl}(3/2^+)$	0	0	0	3.742	3.740	3.752	97.29	97.24	98.23	[23]	
		2.625	2.638	2.645	5.015	4.963	>5.8	0.24	0.26	<0.03		
		3.946	4.024	2.693	4.949	4.911	4.989	0.008	0.006	0.16		
		4.765	4.833	3.918	5.235	5.174	4.88	0.001	$1 \cdot 10^{-4}$	0.01		
${}^{35}\text{Cl}(1/2^+)$		1.225	1.237	1.219	5.127	5.088	5.091	1.59	1.63	1.23		
		3.980	4.055	3.967	4.839	4.830	4.81	0.009	0.006	0.007		
${}^{35}\text{Cl}(5/2^+)$		1.677	1.657	1.763	5.167	5.160	5.475	0.81	0.8	0.24		
		3.096	3.092	3.002	5.395	5.344	4.973	0.03	0.04	0.08		
${}^{35}\text{K}((3/2)^+)$	${}^{35}\text{Ar}(3/2^+)$	0	0	0	4.942	4.920	5.07	37.49	37.59	19	[19]	
		2.625	2.638	2.638	6.360	7.167	≥ 6.2	0.34	0.41	≤ 0.4		
		3.946	4.024	4.065	6.360	7.167	5.64	0.03	0.02	0.55		
${}^{35}\text{Ar}(1/2^+)$		1.225	1.237	1.184	7.791	7.769	5.77	0.02	0.02	2.2		
		3.980	4.055	4.528	4.876	4.876	4.85	4.56	4.18	0.7		
${}^{35}\text{Ar}(5/2^+)$		1.677	1.657	1.750	4.787	4.782	4.91	22	21.71	11.9		
		3.096	3.092	2.982	4.302	4.266	4.27	30.3	31.86	26		
${}^{36}\text{K}(2^+)$	${}^{36}\text{Ar}(2^+)$	1.818	1.814	1.970	4.671	4.659	4.78	73.02	74.32	44	[32]	
		4.254	4.319	4.441	4.662	4.634	4.9	25.10	25.13	8.4		
		6.375	6.441	4.950	5.862	5.769	6.48	0.47	0.54	0.16		
${}^{37}\text{K}(3/2^+)$	${}^{37}\text{Ar}(3/2^+)$	0	0	0	3.655	3.646	3.657	97.21	96.87	97.88	[20]	
		3.653	3.693	3.601	4.913	4.889	4.958	0.02	0.02	0.02		
		4.845	4.857	3.937	5.357	5.347	5.8	$1 \cdot 10^{-4}$	$1 \cdot 10^{-4}$	0.001		
${}^{37}\text{Ar}(1/2^+)$		1.386	1.362	1.409	6.712	6.655	7.38	0.03	0.02	0.004		
		2.771	2.756	2.796	3.900	3.797	3.785	2.22	2.71	2.06		
${}^{37}\text{Ar}(5/2^+)$		3.155	3.129	3.169	4.201	4.356	6.34	0.51	0.35	0.002		
${}^{38}\text{K}(3^+)$	${}^{38}\text{Ar}(2^+)$	1.843	1.850	2.167	4.707	4.684	4.975	92.65	92.64	99.84	[47]	
		4.239	4.221	3.935	6.158	6.237	5.88	0.05	0.04	0.14		
		9.935	10.070	4.565	5.566	5.551	>4.7	0.011	0.011	<0.15		
${}^{36}\text{Ca}(0^+)$	${}^{36}\text{K}(1^+)$	8.759	8.668	5.349	3.484	3.461	>4.6	7.29	7.29	<0.02		
${}^{36}\text{Ca}(0^+)$	${}^{36}\text{K}(1^+)$	1.071	1.063	1.112	4.040	4.039	4.519	47.24	44.59	14.3	[48]	
		1.732	1.732	1.618	4.044	3.975	4.06	33.73	37.06	31		
		2.553	2.578	3.357	3.845	4.879	4.06	3.43	2.92	10.3		
		3.379	3.376	4.450	4.071	4.058	4.29	12.54	12.11	2.6		
		5.591	5.634	4.658	4.672	4.580	4.55	0.63	0.7	1.2		
		6.124	6.111	5.926	3.952	3.888	3.73	2.05	2.25	2.2		
		6.547	6.527	6.787	4.554	4.563	3.900	0.34	0.33	0.5		
${}^{37}\text{Ca}(3/2^+)$	${}^{37}\text{K}(3/2^+)$	0	0	0	4.892	4.890	5.040	27.68	26.83	18.5	[21]	
		3.653	3.693	3.622	4.708	4.648	4.930	5.74	6.18	3.3		
${}^{37}\text{K}(1/2^+)$		1.386	1.362	1.370	5.092	5.082	5.690	8.94	8.97	2.14		
		4.265	4.287	4.192	4.063	4.043	6.330	16.47	16.39	0.09		
${}^{37}\text{K}(5/2^+)$		2.771	2.756	2.750	4.161	4.170	4.790	35.38	33.82	7.9		
		3.155	3.129	3.239	5.799	5.254	4.900	0.64	2.21	4.5		
${}^{38}\text{Ca}(0^+)$	${}^{38}\text{K}(1^+)$	0.538	0.546	0.458	4.919	4.906	4.800	3.686	3.51	2.84	[22]	
		1.504	1.464	1.697	3.450	3.417	3.426	46.02	48.22	19.47		
		4.221	4.201	3.341	3.859	3.865	4.160	0.40	0.39	0.34		
		5.578	5.573	3.855	7.803	7.789	4.800	$1 \cdot 10^{-5}$	$1 \cdot 10^{-5}$	0.02		
		6.665	6.587	3.976	3.778	3.780	4.050	$6 \cdot 10^{-4}$	$1 \cdot 10^{-5}$	0.11		
		11.026	10.906	4.174	3.576	3.566	5.300	$1 \cdot 10^{-5}$	$1 \cdot 10^{-5}$	$1 \cdot 10^{-4}$		
${}^{39}\text{Ca}(3/2^+)$	${}^{39}\text{K}(3/2^+)$	0	0	0	3.596	3.591	3.630	99.96	99.96	99.92	[49]	
		2.648	2.633	2.522	3.799	3.799	7.0004	0.0004	0	0.002		

Table 4. The superallowed transitions($0^+ \rightarrow 0^+$) are listed for the concerned nuclei. The theoretical $\log ft$ values and branching ratios of β^+ /EC decay of the concerned nuclei are compared with the experimental data. The experimental ground state energy and parity J^π of the parent and daughter nucleus are listed along with Q values; the references to the experimental data are given in the last column; J_P^π (J_D^π) and E_P (E_D) are spin-parity and excitation energy of parent (daughter) nuclei, respectively.

Nuclide	Decay	Q(keV)	E_P (keV)	J_P^π	E_D (keV)	J_D^π	$\log ft$			Branch (%)			Ref.
							USDB	SDNN	Expt.	USDB	SDNN	Expt.	
^{18}Ne	β^+ /EC	4445.7	0	0^+	1041.5	0^+	3.497	3.497	3.468	4.95	4.95	7.69	[7]
^{22}Mg	β^+ /EC	4781.6	0	0^+	657	0^+	3.497	3.497	3.487	26.2	25.25	53.21	[8]
^{26}Si	β^+ /EC	5069.14	0	0^+	228.3	0^+	3.497	3.497	3.490	31.48	31.99	75.05	[10]
^{30}S	β^+ /EC	6138	0	0^+	677.01	0^+	3.523	3.523	3.485	67.15	68.77	76.14	[6]
^{32}Ar	β^+ /EC	11134.7	0	0^+	5046.3	0^+	7.507	7.507	3.179	0.02	0.014	22.70	[16]
^{34}Ar	β^+ /EC	6061.83	0	0^+	0.0	0^+	3.636	3.636	3.485	76.17	76.11	94.46	[17]
^{38}Ca	β^+ /EC	6742.26	0	0^+	130.2	0^+	3.497	3.497	3.487	49.87	47.85	77.19	[22]

Table 5. The theoretical β^+ /EC -decay half-lives are compared with the experimental data for the concerned nuclei; the experimental Q values; $\beta^+ + \epsilon$ -decay probabilities; quenched theoretical sum $B(GT)$ values.

$^A Z_i (J^\pi)$	$^A Z_f$	Q value (keV)	Sum $B(GT)$		β -decay half-life			$\beta^+ + \epsilon$ %
			USDB	SDNN	USDB	SDNN	EXPT.	
$^{18}\text{Ne}(0^+)$	^{18}F	4445.7 \pm 47	3.229	3.336	1.645 s	1.559 s	1.672 \pm 8 s[7]	100
$^{19}\text{Ne}(1/2^+)$	^{19}F	3238.4 \pm 6	1.693	1.753	18.224 s	17.252 s	17.22 \pm 2 s[41]	100
$^{20}\text{Na}(2^+)$	^{20}Ne	13886 \pm 7	1.583	1.606	221.6 ms	215.02 ms	447.9 \pm 23 ms[32]	100
$^{21}\text{Na}(3/2^+)$	^{21}Ne	3547.14 \pm 28	0.462	0.469	29.568 s	27.756 s	22.49 \pm 4 s[6]	100
$^{22}\text{Na}(3^+)$	^{22}Ne	2843.20 \pm 17	0.00024	0.00038	1.57 y	0.99 y	2.6018 \pm 22 y[42]	100
$^{21}\text{Mg}(5/2^+)$	^{21}Na	13098 \pm 16	0.130	0.128	170.8 ms	163.02 ms	122 \pm 3 ms[9]	100
$^{22}\text{Mg}(0^+)$	^{22}Na	4781.6 \pm 3	2.174	2.305	2.93 s	2.696 s	3.875 \pm 12 s[8]	100
$^{23}\text{Mg}(3/2^+)$	^{23}Na	4056.17 \pm 32	0.380	0.381	16.38 s	15.69 s	11.304 \pm 45 s[11]	100
$^{22}\text{Al}(4^+)$	^{22}Mg	17560	0.155	0.159	56.34 ms	50.71 ms	91.1 \pm 5 ms[12]	100
$^{23}\text{Al}(5/2^+)$	^{23}Mg	12221.6 \pm 4	1.449	1.661	813.69 ms	715.6 ms	446 \pm 6 ms[43]	100
$^{24}\text{Al}(4^+)$	^{24}Mg	13884.77 \pm 4	0.005	0.006	2.481 s	1.994 s	2.053 \pm 4 s[13]	100
$^{25}\text{Al}(5/2^+)$	^{25}Mg	4276.7 \pm 5	0.519	0.531	9.63 s	9.206 s	7.183 \pm 12 s[6]	100
$^{25}\text{Si}(5/2^+)$	^{25}Al	12740 \pm 10	1.705	0.879	238.7 ms	218.7 ms	220 \pm 3 ms[14]	100
$^{26}\text{Si}(0^+)$	^{26}Al	5069.14 \pm 8	1.834	1.987	1.495 s	1.441 s	2.245 \pm 7 s[6]	100
$^{27}\text{Si}(5/2^+)$	^{27}Al	4812.36 \pm 10	0.635	0.624	5.63 s	5.46 s	4.16 \pm 4 s[15]	100
$^{26}\text{P}(3^+)$	^{26}Si	18258 \pm 90	0.190	0.200	43.13 s	42.11 s	43.7 \pm 6 ms[44]	100
$^{28}\text{P}(3^+)$	^{28}Si	14345.1 \pm 12	0.162	0.160	154.45 ms	152.02 ms	270.3 \pm 5 ms[44]	100
$^{29}\text{P}(1/2^+)$	^{29}Si	4942.5 \pm 6	0.503	0.521	9.37 s	9.256 s	8.862 \pm 15 s[6]	100
$^{30}\text{P}(1^+)$	^{30}Si	4232.4 \pm 3	0.207	0.209	3.04 min	3.26 min	2.498 \pm 4 min[6]	100
$^{29}\text{S}(5/2^+)$	^{29}P	13795 \pm 50	0.219	0.232	119.69 ms	126.79 ms	188 \pm 4 ms[45]	100
$^{30}\text{S}(0^+)$	^{30}P	6138 \pm 3	1.123	1.286	1.813 s	1.761 s	1.178 \pm 5 s[6]	100
$^{31}\text{S}(1/2^+)$	^{31}P	5398.01 \pm 23	0.422	0.430	3.575 s	3.441 s	2.553 \pm 18 s[6]	100
$^{31}\text{Cl}(3/2^+)$	^{31}S	12008 \pm 3	0.442	0.402	257.19 ms	251.94 ms	190 \pm 1 ms[18]	100
$^{33}\text{Cl}(3/2^+)$	^{33}S	5582.59 \pm 44	0.614	0.462	3.387 s	3.322 s	2.511 \pm 3 s[6]	100
$^{34}\text{Cl}(3^+)$	^{34}S	5491.63 \pm 43	0.150	0.163	29.89 min	27.35 min	31.99 \pm 3 min[46]	100
$^{32}\text{Ar}(0^+)$	^{32}Cl	11134.7 \pm 20	3.695	4.066	111.81 ms	104.24 ms	98 \pm 2 ms[16]	100
$^{33}\text{Ar}(1/2^+)$	^{33}Cl	11619.1 \pm 6	0.476	0.483	217.67 ms	206.87 ms	173.0 \pm 20 ms[38]	100
$^{34}\text{Ar}(0^+)$	^{34}Cl	6061.83 \pm 8	1.168	1.280	1580.68 ms	1497.39 ms	843.8 \pm 4 ms[17]	100
$^{35}\text{Ar}(3/2^+)$	^{35}Cl	5966.1 \pm 7	0.310	0.324	2.501 s	2.383 s	1.775 \pm 7 s[23]	100
$^{35}\text{K}((3/2)^+)$	^{35}Ar	11874.5 \pm 9	0.348	0.358	258.92 ms	246.47 ms	178 \pm 8 ms[19]	100
$^{36}\text{K}(2^+)$	^{36}Ar	12814.21 \pm 35	0.205	0.188	181.66 ms	177.91 ms	342 \pm 2 ms[32]	100
$^{37}\text{K}(3/2^+)$	^{37}Ar	6147.48 \pm 23	1.017	1.073	1.624 s	1.523 s	1.225 \pm 7 s[20]	100
$^{38}\text{K}(3^+)$	^{38}Ar	5914.07 \pm 4	1.333	1.376	3.87 min	3.67 min	7.651 \pm 19 min[47]	100
$^{36}\text{Ca}(0^+)$	^{36}K	10966 \pm 40	2.165	1.795	46.94 ms	59.37 ms	101.2 \pm 20 ms[48]	100
$^{37}\text{Ca}(3/2^+)$	^{37}K	11664.5 \pm 8	0.953	0.995	184.99 ms	176.06 ms	181.1 \pm 10 ms[21]	100
$^{38}\text{Ca}(0^+)$	^{38}K	6742.26 \pm 6	3.655	3.779	493.30 ms	448.71 ms	443.76 \pm 35 ms[22]	100
$^{39}\text{Ca}(3/2^+)$	^{39}K	6524.5 \pm 6	1.839	1.901	1007.24 ms	954.49ms	860.3 \pm 10 ms[49]	100

Table 2 contains the calculated phase space factors for β^+ and EC decay only for those nuclei that have significant EC phase space factors. The table reflects that the EC phase space factors play an essential role in the decay process where the Q -values are equal to or less than 2 MeV. In this work, we have included the β^+ /EC decay phase space factor in the half-life calculations.

The total β^+ /EC -decay half-life is calculated using the partial half-lives of all the transitions. So, to better understand the nuclear β -decay, we have to analyze the details of each transition. The experimental data with theoretical shell-model results of excitation energies and β^+ -decay properties like $\log ft$ values, branching percentages of 37 proton-rich and $N = Z$ nuclei of sd shell are compared in Table 3. The initial and final nuclei and the spin parity, are in columns 1 and 2, respectively. The theoretical results using USDB, SDNN and experimental excitation energies (in keV) of each state involved in β^+ -decays are reported in columns 3, 4, and 5, respectively. Columns 6, 7 and 8 reported the theoretical results using USDB, SDNN and experimental $\log ft$ values, respectively. The Eq. 15 has been used to calculate theoretical branching fractions. Columns 9 and 10 represent theoretical results using USDB and SDNN interactions, respectively, and the experimental values are listed in column 11. The rms deviation of the excitation energy between theory and experiment is 1281 keV, and the average relative error is 13.06% for USDB interaction, and for SDNN interaction, the rms deviation is 1362 keV with an average relative error of 14.06%. Overall, the excitation energies predicted by USDB interaction are closer to the experimental data than those predicted by SDNN interaction.

In [40], the $\log ft$ values are reported using shell-model for the β^+ -decay of ^{37}K nucleus, the $\log ft$ values are 3.53, 6.32, and 3.41 for the transitions at $3/2^+$, $1/2^+$, and $5/2^+$, respectively. In the present work, the SM results are 3.655, 6.712, and 3.9 using USDB and 3.646, 6.655, and 3.797 using SDNN interactions for the transitions at $3/2^+$, $1/2^+$, and $5/2^+$, respectively. Our theoretical quenched $\log ft$ values are closer to the experimental values 3.657, 7.38, and 3.785 for the transitions at $3/2^+$, $1/2^+$, and $5/2^+$, respectively. The observed weak branching fractions in ^{20}Na , ^{30}P , ^{33}Cl , ^{37}K , ^{38}K , and ^{38}Ca are successfully reproduced by shell model calculation using USDB and SDNN interactions. Overall, the shell model results for sd shell nuclei agree with the experimental data for excitation energies, $\log ft$ values and the branching ratios. There are a few cases where the theoretical results deviated from the experimental data.

The seven superallowed transitions with $0^+ \rightarrow 0^+$ for ^{18}Ne , ^{22}Mg , ^{26}Si , ^{30}S , ^{32}Ar , ^{34}Ar , and ^{38}Ca are reported in Table 4. We have also included the superallowed transitions in the β -decay half-lives calculation. From Table 4, the theoretical results of $\log ft$ values are in good agreement with the experimental data except for ^{32}Ar . In the case of ^{32}Ar , the calculated $\log ft$ values are larger than the experimental one; this is because the calculated Fermi matrix element is small; hence, Fermi reduced transition probability $B(F)$ is small, and hence $\log ft$ value is large.

Due to the large $\log ft$ value, the branching ratio is smaller in this case. Overall, the branching ratios for the superallowed transitions agree with the experimental data.

The theoretical and the experimental β -decay half-lives of the concerned nuclei are compared in Table 5. The β^+ /EC -decay half-lives are displayed in the log frame in Fig.2. The experimental Q -values, $\beta^+ + \epsilon$ (electron capture) decay probabilities and the quenched theoretical sum $B(GT)$ values are also reported in Table 5. For all 37 nuclei, their observed probabilities of $\beta^+ + \epsilon$ -decay are 100%. The parent and daughter nuclei are listed in the first and second columns. Column 3 presents the experimental Q -values taken from [32]. The sums of quenched $B(GT)$ values are presented in columns 4 and 5. The theoretical (quenched) β -decay half-lives are presented in columns 6 and 7 for USDB and SDNN interactions, respectively, while the experimental data are given in column 8. The last column represents the experimental probabilities of $\beta^+ + \epsilon$ decay. The average relative error of the theoretical β^+ /EC -decays half-lives is 33.1% for USDB interaction while 29.3% for SDNN interaction. For Ne, both the interactions predict the relative error less than 5%, while other nuclei exhibit higher relative errors. The relative errors for nuclei such as ^{18}Ne , ^{19}Ne , ^{24}Al , ^{25}Si , ^{26}P , ^{29}P , ^{34}Cl , ^{32}Ar , ^{37}Ca , ^{38}Ca , and ^{39}Ca are all below or equal to 20%. For ^{34}Ar , ^{36}K , and ^{36}Ca , the theoretical results are quite different from the experimental data. It might be because of two reasons: either the ground state angular momentum is not predicted correctly, or the used Q -values have large uncertainties. This leads to errors in the theoretical half-lives calculations. A comparative analysis of β^+ /EC -decay half-lives between USDB and SDNN interactions show that the theoretical results for the SDNN interaction with a quenching factor of 0.815 exhibits closer results than those of the USDB interaction, which has a quenching factor of 0.794.

We included the electron capture phase space factor using Eq. 12, and 13 in the calculations of beta decay half-lives. For instance, in the case of ^{29}P , the initial half-lives were calculated to be 9.265 and 8.871 s. After incorporating EC, these values changed to 9.256 and 8.863 s, respectively. This indicates that the results from SDNN interaction is closer to the experimental half-life 8.862 s than USDB interaction. The influence of the EC phase space factor is relatively small in the cases of ^{22}Na , ^{23}Mg , ^{30}P , ^{34}Cl , and ^{38}K . In the absence of electron capture, the half-life of ^{22}Na are 1.75 and 1.10 y for USDB and SDNN interactions, respectively. However, after considering the EC phase space factor, the half-life become 1.58 and 0.98 y for USDB and SDNN interactions, respectively, while the experimental data is 2.6018 y. Excluding the EC phase space factor, the half-life of ^{23}Mg was determined to be 16.39 and 15.70 s for the USDB and SDNN, respectively when the EC factor was taken into account, the half-life changed to 16.38 and 15.69 s, where as the experimental half-life is 11.304 s. Similarly, for ^{30}P , both USDB and SDNN interactions demonstrated a slight change. Initially, the half-life without EC was 3.040 and 3.261 min for USDB and SDNN interactions, respectively. Upon includ-

ing EC, the half-life become 3.036 and 3.057 min in both cases, while observed half-life of ^{30}P is 2.498 min. In ^{34}Cl , without EC, the half-life is 30.21 min for USDB and 27.63 min for SDNN interaction. With the inclusion of the EC phase space factor, the half-life became 29.89 and 27.35 min, respectively, whereas, the experimental half-life of ^{34}Cl is 31.99 min. Similarly, for ^{38}K , the half-life without EC inclusion is 3.885 and 3.684 min for USDB and SDNN, respectively. Incorporating the EC phase space factor the half-life would become 3.868 and 3.668 min for USDB and SDNN interaction, respectively, while the observed half-life is 7.651 min, a significant difference is found between theoretical and experimental half-life. The EC phase space factor contributions can improve the half-life if we considered the additional corrections arise from the screening of the nuclear charge by atomic electrons and from the finite nuclear size in Eq. 13. In general, the EC phase space factor influences the decay half-life of some nuclei more significantly than others due to the variations in energy available for the decay (Q -value), atomic orbital density, imperfect atomic wave function overlap in the initial and final state of decay, environmental factors such as temperature, pressure, etc. which tends to change the electron density, type of decay, relativistic effect which comes into play at higher atomic number $Z > 70$. It is also depends on the forbiddenness of the decay, in the present study we only consider allowed transitions so this effect can be ignore.

The SM results of $\log ft$ values, branching ratios, and half-lives of ^{25}Si , and ^{26}P in sd space using USD interaction are reported in ref. [14]. In [14], The theoretical half-lives of ^{25}Si , and ^{26}P are reported as 216.1 and 40.85 ms respectively, while the measured values are 220(3) and 43.7(6) ms respectively. In the present work, the half-lives using USDB and SDNN interactions are 238.7 and 218.7 ms for ^{25}Si and 43.13 and 42.11 s for ^{26}P . Our results for half-lives of ^{26}P are more closer to the experimental data than previous SM results, while for ^{25}Si the SDNN prediction is more closer to the observed value.

The half-life of ^{22}Al has been calculated using two different Q -values reported in [12] and [50]. A significant difference have been observed when using different Q -values. When using a Q -values of 18.601 MeV [50] a quenched half-life of 45 and 41.67 ms have been obtained for USDB and SDNN interactions, respectively. However when a Q -values of 17.56 MeV [12] is used, a significant improvement have been seen in both USDB and SDNN interactions with half-life of 56.34 and 50.71 ms, respectively.

A superallowed transitions with $0^+ \rightarrow 0^+$ for ^{36}Ca observed at 4281.9 keV with branching ratio 38.03%. The calculated Fermi matrix element (M_F) for the transition $0^+ \rightarrow 0^+$ are 4.04×10^{-5} using USDB and 4×10^{-5} using SDNN interactions respectively, and the corresponding Fermi reduced transition probability ($B(F)$) are 1.63×10^{-9} and 1.6×10^{-9} . Due to small Fermi reduced transition probability the half-life contribution from superallowed transition is negligible and hence a significant difference between theory and experiment are observed for ^{36}Ca .

The ratios between theoretical β^+ -decay half-lives and experimental data for the concerned nuclei are plotted in

Fig.3. For the majority of the isotopes, the ratios between theoretical β^+ -decay half-lives and experimental values are distributed quite close to unity.

Fig. 4 shows β^+ -decay Q -values between theoretical results using Eq. 16 and the experimental data from ref. [32]. The figure shows a recurring pattern: as the mass number of a particular isotope increases, the associated Q -value decreases. Moving towards lower Q -values in beta decay signifies an approach to more stable nuclei. The Q -value behaviour for each β^+ -decay exhibits a consistent pattern in both interactions, which resembles the experimental outcomes. Moreover, the Q -value for each β^+ -decay is slightly lower than the experimental data. The rms deviation of Q -value between theory and the experiment is 880.4 keV, and the average relative error is 13.55% for USDB interaction, while for SDNN interaction, the rms deviation is 886.4 keV with 13.6% average relative error. For Al and Ca, the relative error of the theoretical Q -values is less than 10%, and for Ne and Na, it is greater than 20%, and for the rest of the nuclei (Mg, Si, P, S, Cl, Ar and K), the relative error lies in between 10 - 20%.

4 Summary and Conclusion

In the present work, we have reported a systematic SM study of β^+/EC -decay half-lives, $\log ft$ values, branching fractions and Q -values. The calculations have been performed in full sd model space using two different USDB and SDNN interactions. We have also reported the quenching factor for sd space using USDB and SDNN interactions with Gamow Teller matrix elements for 116 decays. Further, the β^+/EC -decay properties are calculated with axial-vector coupling constant $g_A (= 1.27)$, and κ value ($= 6289$). We have also included superallowed $0^+ \rightarrow 0^+$ transition for seven nuclei and the electron phase space factor for the required nuclei in β -decay half-lives calculations. Overall, the calculated results of excitation energies, $\log ft$ values, quenched half-lives, and branching fractions are in reasonable agreement with the available experimental data. The present shell model results of β^+/EC -decay half-lives, $\log ft$ values, branching ratios, Q -values for the sd shell nuclei will add more information to the earlier experimental works, and the calculated average quenching factors in this work can be used for half-life calculations in sd shell.

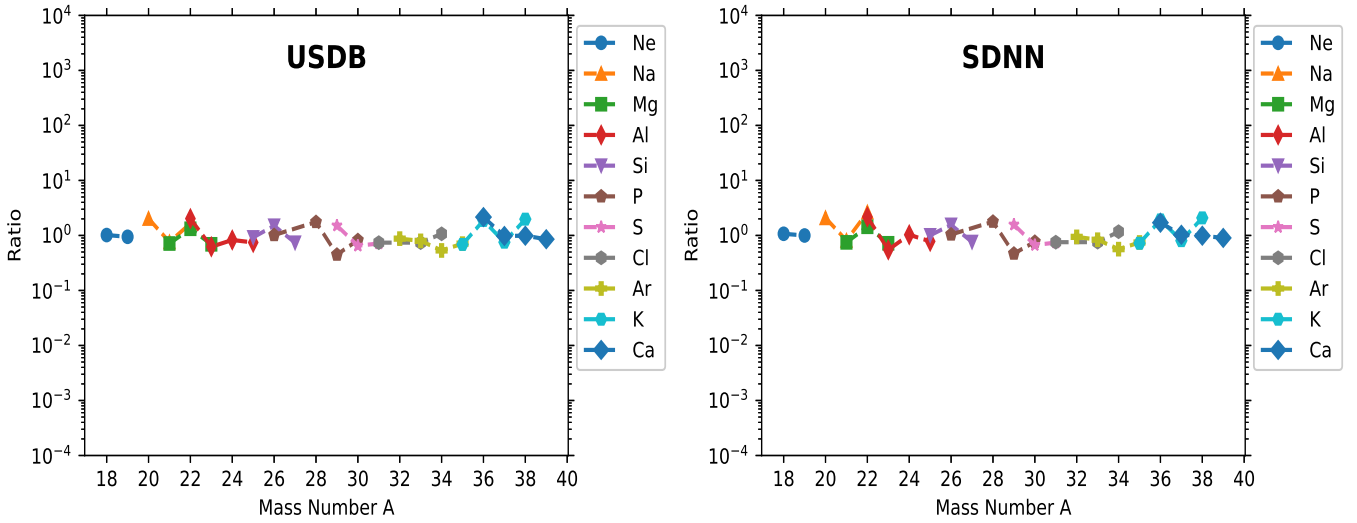


Fig. 3. The theoretical to experimental half-lives ratios versus the mass number A for the concerned sd shell nuclei.

Acknowledgment:

Surender acknowledges financial support from BHU for his PhD thesis work. V. Kumar acknowledges financial support from IoE Seed Grant BHU (R/Dev/D/IoE/Seed Grant-II/2021-22/39960), and SERB Project (File No. EEQ/2023/000157), Govt. of India.

References

1. P. Gysbers *et al.*, ‘Discrepancy between experimental and theoretical β -decay rates resolved from first principles’, *Nat. Phys.* **15** 428 (2019).
2. A. Algora *et al.*, ‘Beta-decay studies for applied and basic nuclear physics’, *Eur. Phys. J. A* **57** 85 (2021).
3. B. Rubio *et al.*, ‘Beta decay studies with total absorption spectroscopy and the Lucrecia spectrometer at ISOLDE’ *J. Phys. G: Nucl. Part. Phys.* **44** 084004 (2017).
4. T. Otsuka *et al.*, ‘Monte Carlo shell model for atomic nuclei’ *Prog. Part. Nucl. Phys.* **47** 319 (2001).
5. S. Akkoyun *et al.*, ‘Improvement Studies of an Effective Interaction for $N = Z$ sd -Shell Nuclei by Neural Networks’ *Bulg. J. Phys.* **48** 245 (2021).
6. H. S. Wilson, R. W. Kavanagh and F. M. Mann, ‘Gamow-Teller transitions in some intermediate-mass nuclei’ *Phys. Rev. C* **22** 1696 (1980).
7. E. G. Adelberger *et al.*, ‘Beta decays of ^{18}Ne and ^{19}Ne and their relation to parity mixing in ^{18}F and ^{19}F ’, *Phys. Rev. C* **27** 2833 (1983).
8. N. L. Achouri *et al.*, ‘The β - γ decay of ^{21}Na ’, *J. Phys. G: Nucl. Part. Phys.* **37** 045103 (2010).
9. R. G. Sextro *et al.*, ‘Isospin-forbidden particle decays in light nuclei’, *Nucl. Phys. A* **273** 477 (1976).
10. J. C. Hardy, H. Schmeing, J. S. Geiger, R.L. Graham, ‘The superallowed β -decay of ^{18}Ne , ^{22}Mg and ^{26}Si ’, *Nucl. Phys. A* **246** 61 (1975).
11. C. Magron *et al.*, ‘Precise measurements of half-lives and branching ratios for the mirror transitions in the decay of ^{23}Mg and ^{27}Si ’, *Eur. Phys. J. A* **53** 77 (2017).
12. N. L. Achouri *et al.*, ‘The β -decay of ^{22}Al ’, *Eur. Phys. J. A* **27** 287 (2006).
13. E. K. Warburton, C. J. Lister, D. E. Alburger, and J. W. Olness, ‘Beta decay of ^{24}Al ’, *Phys. Rev. C* **23** 1242 (1981).
14. J. C. Thomas *et al.*, ‘Beta-decay properties of ^{25}Si and ^{26}P ’, *Eur. Phys. J. A* **21** 419 (2004).
15. W. W. Daehnick and R. D. Rosa, ‘Weak branches in ^{42}Sc , ^{35}Ar , and ^{27}Si β^+ -decay’, *Phys. Rev. C* **31** 1499 (1985).
16. M. Bhattacharya *et al.*, ‘ ft value of the $0^+ \rightarrow 0^+$ β^+ decay of ^{32}Ar : A measurement of isospin symmetry breaking in a superallowed decay’, *Phys. Rev. C* **77** 065503 (2008).
17. J. C. Hardy and I. S. Towner, ‘Superallowed $0^+ \rightarrow 0^+$ beta-decay from $T_z = -1$ sd -shell nuclei’, *J. Phys.: Conf. Ser.* **387** 012006 (2012).
18. M. B. Bennett *et al.*, ‘Detailed study of the decay ^{31}Cl ($\beta\gamma$) ^{31}S ’, *Phys. Rev. C* **97** 065803 (2018).
19. G. T. Ewan *et al.*, ‘The decay of ^{35}K ’, *Nucl. Phys. A* **343** 109 (1980).
20. E. Hagberg *et al.*, ‘Measurement of the l-forbidden Gamow-Teller branch of ^{37}K ’, *Phys. Rev. C* **56** 135 (1997).
21. N. I. Kaloskamis *et al.*, ‘Isospin mixing in ^{37}K and spin decomposition of Gamow-Teller strength in ^{37}Ca decay’, *Phys. Rev. C* **55** 640 (1997).
22. B. Blank *et al.*, ‘Half-life and branching ratios for the β decay of ^{38}Ca ’, *Eur. Phys. J. A* **51** 8 (2015).
23. E. G. Adelberger *et al.*, ‘The l-forbidden Gamow-Teller decay of ^{39}Ca ’ *Nucl. Phys. A* **417** 269 (1984).
24. V. Kumar, P. C. Srivastava and H. Li, ‘Nuclear β^- -decay half-lives for fp and fp_g shell nuclei’ *J. Phys. G: Nucl. Part. Phys.* **43** 105104 (2016).
25. V. Kumar and P. C. Srivastava, ‘Shell model description of Gamow-Teller strengths in pf -shell nuclei’, *Eur. Phys. J. A* **52** 181 (2016).
26. V. Kumar, A. Kumar and P. C. Srivastava, ‘Shell-model study for GT-strengths corresponding to β -decay of ^{60}Ge and ^{62}Ge ’, *Nucl. Phys. A* **1017** 122344 (2022).
27. V. Kumar and P. C. Srivastava, ‘Shell-model study of β^+ /EC-decay half-lives for $Z=20-30$ nuclei’ *Eur. Phys. J. A* **59** 237 (2023).

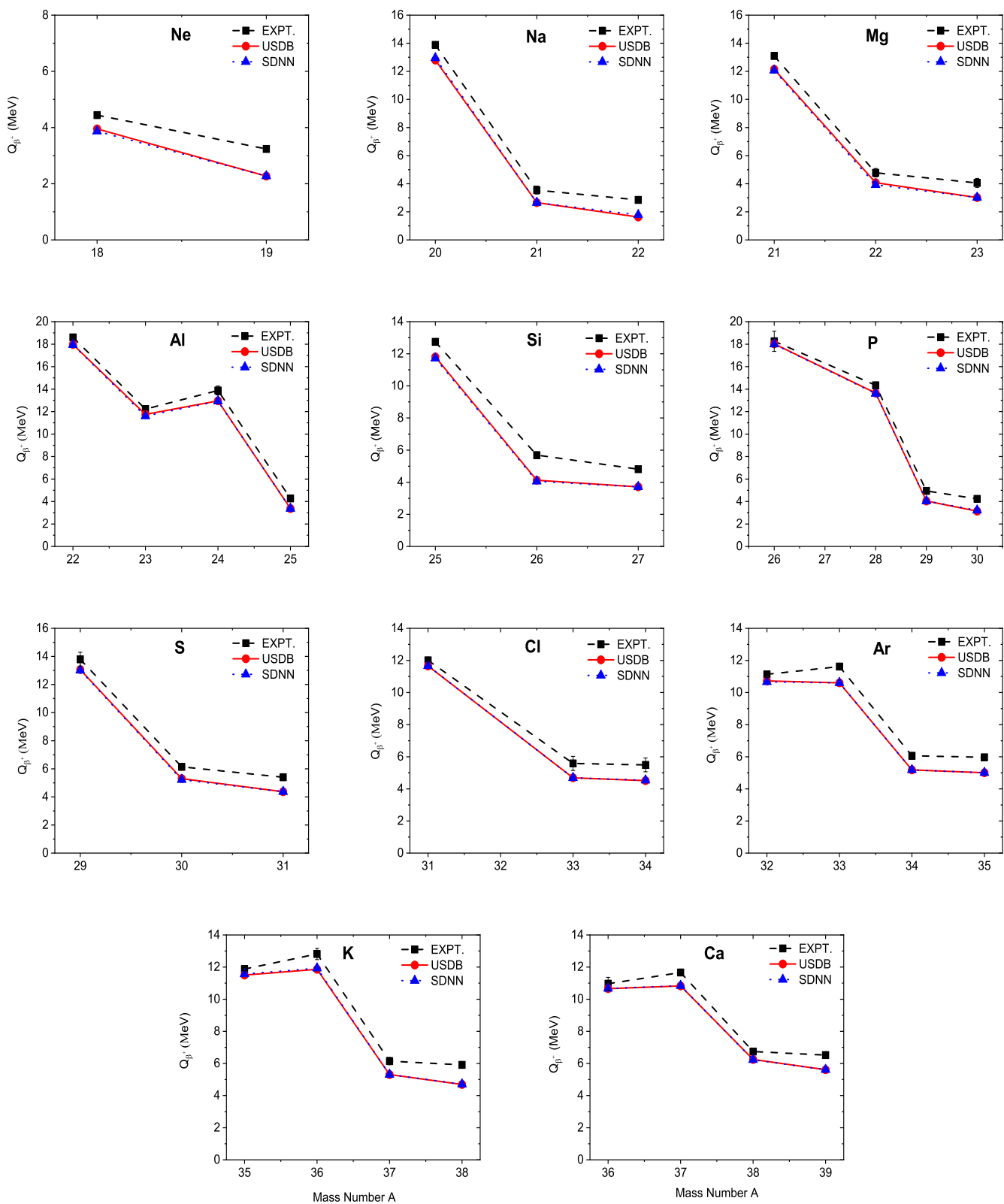


Fig. 4. The theoretical and experimental Q values versus mass number A of the concerned sd shell nuclei.

28. G. Martínez-Pinedo *et al.*, ‘Effective g_A in the fp shell’, *Phys. Rev. C* **53** R2602 (1996).
29. B. A. Brown and B. H. Wildenthal, ‘Experimental and theoretical Gamow-teller beta-decay observables for the *sd* shell nuclei’, *At. Data Nucl. Data Tables* **33**, 347 (1985).
30. C. Patrignani and Particle Data Group, *Rev. Part. Phys., Chin. Phys. C*, **40** 100001 (2016).
31. J. Suhonen, *From Nucleons to Nucleus: Concepts of Microscopic Nuclear Theory* (Springer, Berlin, 2007).
32. ENSDF database, <http://www.nndc.bnl.gov/ensdf/>.
33. S. Sharma, P. C. Srivastava, A. Kumar, and T. Suzuki, ‘Shell-model description for the properties of the forbidden β^- -decay in the region “northeast” of ^{208}Pb ’, *Phys. Rev. C* **106** 024333 (2022).
34. E. Caurier *et al.*, ‘Full $0\hbar\omega$ shell model calculation of the binding energies of the $1f_{7/2}$ nuclei’ *Phys. Rev. C* **59** 2033 (1999).
35. B. Alex Brown and W. A. Richter, ‘New “USD” Hamiltonians for the *sd* shell’, *Phys. Rev. C* **74** 034315 (2016).
36. B. A. Brown, W. D. M. Rae, E. McDonald, and M. Horoi, ‘The Shell-Model Code NuShellX@MSU’, *NuShellX@MSU*.
37. B. H. Wildenthal, ‘Empirical strengths of spin operators in nuclei’, *Prog. Part. Nucl. Phys.* **11** 5 (1984).
38. N. Adimi *et al.*, ‘Detailed β -decay study of ^{33}Ar ’, *Phys. Rev. C* **81** 024311 (2010).
39. B. H. Wildenthal, M. S. Curtin, and B. A. Brown, ‘Predicted features of the beta decay of neutron-rich *sd*-shell nuclei’, *Phys. Rev. C* **28** 1343 (1983).
40. B. H. Wildenthal *et al.*, ‘Calculations with a $1s$, $0d$ Shell Model for $A = 34 - 38$ Nuclei’, *Phys. Rev. C* **4** 1266 (1971).
41. F. Ajzenberg-Selove, ‘Energy levels of light nuclei $A = 18-20$ ’, *Nucl. Phys. A* **475** 1 (1987).
42. M. P. Silverman and W. Strange, ‘Search for correlated fluctuations in the β^+ decay of Na-22 ’ *Euro. Phys. Lett.* **87** 32001 (2009).
43. A. Saastamoinen *et al.*, ‘Experimental study of beta-delayed proton decay of Al-23 for nucleosynthesis in novae’, *Phys. Rev. C* **83** 1 (2011).
44. T. J. Ognibene, J. Powell, D. M. Moltz, M. W. Rowe, and Joseph Cerny, Additional results from the β -delayed proton decays of ^{27}P and ^{31}Cl ’, *Phys. Rev. C* **54**, 1098 (1996).
45. D. J. Vieira, R. A. Gough, and Joseph Cerny, β -delayed proton decay of ^{29}S ’, *Phys. Rev. C* **19** 177 (1979).
46. Th. Krüger, H. Appel, W.-G. Thies, H. Behrens, ‘Spectrum shape studies of the β -transitions $^{34m}\text{Cl}(3^+ \rightarrow 2^+)^{34}\text{S}$ and $^{34}\text{Cl}(0^+ \rightarrow 0^+)^{34}\text{S}$ ’, *Phys. Lett. B* **121**, 303 (1983).
47. F. M. Mann, H. S. Wilson, R. W. Kavanagh, ‘Positron decays of ^{25}Al , ^{37}K , ^{38}K and ^{39}Ca ’, *Nucl. Phys. A* **258**, 341 (1976).
48. López Jiménez *et al.*, ‘New transitions in the β -decay of ^{36}Ca ’, *Eur. Phys. J. A* **10** 119 (2001).
49. E. Hagberg *et al.*, ‘Confirmation of the 1-forbidden Gamow-Teller decay branch of ^{39}Ca ’, *Nucl. Phys. A* **571** 555 (1994).
50. G. Audi *et al.*, ‘The NUBASE evaluation of nuclear and decay properties’, *Nucl. Phys. A* **729**, 3 (2003).